



Get Clarity On Generics

Cost-Effective CT & MRI Contrast Agents

**FRESENIUS
KABI**

[WATCH VIDEO](#)

AJNR

Local Cerebral Blood Flow Measured by CT After Stable Xenon Inhalation

John Stirling Meyer, L. Anne Hayman, Masahiro Yamamoto,
Fumihiko Sakai and Shinji Nakajima

AJNR Am J Neuroradiol 1980, 1 (3) 213-225

<http://www.ajnr.org/content/1/3/213>

This information is current as
of August 14, 2025.

Local Cerebral Blood Flow Measured by CT After Stable Xenon Inhalation

John Stirling Meyer¹
L. Anne Hayman²
Masahiro Yamamoto¹
Fumihiko Sakai¹
Shinji Nakajima¹

A safe, practical, clinically applicable, noninvasive method for measuring local cerebral blood flow (LCBF) using inert xenon (Xe^s) and a 60 sec CT scanner has been developed in the baboon. Direct measurement of expired Xe^s concentration after short inhalation (4–7 min) of 40% Xe^s and the use of computer-programmed autoradiographic formulas allow accurate, reproducible measurements of LCBF using serial 60 sec scans of regions as small as 0.04 cm^3 . LCBF measurements are possible with a single 1 min scan. The method reduces radiation exposure, obviates a costly fourth-generation scanner, avoids anesthetic effects of Xe^s , and reduces the 30 min/scan saturation period. It is less expensive than emission tomography and minimizes problems of overlap and Compton scatter inherent in ^{133}Xe and positron-emission blood flow measurements. Regions of zero perfusion are demonstrable in three dimensions. Tissue solubility and partition coefficients, as well as LCBF, are measured in vivo with high resolution and reproducibility so that minor regional changes in physical properties of tissue that alter solubility are measured. These enhance the potential clinical usefulness of CT scanning.

Measurement of cerebral blood flow using stable xenon (Xe^s) computed tomographic (CT) scanning has been largely confined to animal models for several reasons [1–6]. Anesthetic properties of high concentrations of Xe^s , expense, high radiation dosage from excessive serial scans, time, and personnel necessary for prolonged studies involving immobilized patients have limited clinical implementation. Techniques described here minimize or avoid these adverse factors and combine inherent advantages of Xe^s (an inert gas administered by inhalation, which is diffusible, lipid soluble, and an excellent radiographic contrast agent) with the 3-dimensional resolving powers of CT scanning.

Emission tomography, particularly with the use of short-lived positron-emitting isotopes, has promise for in vivo measurements of metabolism. However, these instruments are expensive and highly specialized, and a cyclotron or powerful generator is necessary to produce the isotopes. Transmission tomography has advantages for measuring local cerebral blood flow (LCBF) compared to external counting of isotopes such as ^{133}Xe . CT scanners are widely available and Compton scatter and overlap are minimized, so that the possibilities for 3-dimensional resolution in vivo are optimal.

Xe^s has been used successfully as a contrast agent during CT scanning of the brain, and its pharmacology and clinical safety are known [1–19]. After prolonged inhalation of high concentrations (80% in oxygen) it has anesthetic properties and may be used for induction of light surgical anesthesia. If lower concentrations (40%–50%) are inhaled and if brief intervals for inhalation are used (about 3–10 min), the anesthetic effects of Xe^s are minimized. After inhalation, Xe^s is freely diffusible through all tissues, particularly brain tissue because of its high lipid solubility [13, 14]. It has an atomic number of 54, compared to 53 for the nondiffusible contrast agent iodine. Both absorb x-rays and give excellent contrast with high resolution on CT scanning [1–6, 15–19].

Xe^s rapidly diffuses across the blood-brain barrier after inhalation to saturate

Received September 10, 1979; accepted after revision January 21, 1980.

This work was supported by stroke center grant NS09287 from the U.S. Public Health Service.

¹Department of Neurology, Baylor College of Medicine, Veterans Administration Medical Center, and Baylor Center for Cerebrovascular Research, Houston, TX. Address reprint requests to J. S. Meyer, Cerebral Blood Flow Laboratory, Veterans Administration Medical Center, 2002 Holcombe Blvd., Houston, TX 77211.

²Department of Radiology, Veterans Administration Medical Center, Houston, TX 77211. Present address: Department of Radiology, University of Texas Health Sciences Center, Houston, TX 77030.

This article appears in May/June 1980 *AJNR* and August 1980 *AJR*.

AJNR 1:213–225, May/June 1980
0195–6108/80/0103–0213 \$00.00
© American Roentgen Ray Society

different tissues of brain in proportion to their fat solubility. Xe^s is thus a potential indicator of both tissue perfusion and tissue solubility. After Xe^s inhalation, changes in regional Hounsfield units (ΔH) measured in normal or abnormal brain tissues by the CT scanner are directly proportional to (1) the percentage concentration of Xe^s inhaled [18]; (2) its solubility in arterial blood; (3) the solubility coefficients and, hence, the partition coefficient between blood and brain (λ) of the normal and abnormal tissues scanned; and (4) local cerebral blood flow. Since many of these variables may be measured or can be controlled, such as the Xe^s concentration inhaled at the time of tissue and blood equilibrium (and hence the concentration of Xe^s in the arterial blood of the end-tidal air), the λ of normal and pathologic tissues may be determined in vivo by recording the ΔH units in the brain tissue when tissue saturation has been reached [5].

In vivo measurements of λ of regional brain tissues are of interest for two reasons:

1. In pathologic regions of brain that become edematous, neoplastic, demyelinated, gliotic, or infarcted, regional λ will be altered, providing in vivo quantitative measurements of physical or chemical changes in brain tissue composition.
2. Knowledge of λ for Xe^s of normal and abnormal tissues in vivo will permit quantitative calculation of regional cerebral blood flow during saturation or desaturation with a precision and resolution not previously possible. Until recently [5] the λ s of pathologic tissues were not measurable in vivo, so that normal λ values were used for calculating LCBF, generating unpredictable errors [20–26].

In the absence of gross pulmonary disease, end-tidal measurements of Xe^s (PEXe^s) during inhalation of the gas are in equilibrium with arterial blood. This permits a noninvasive method for recording the arterial input function of Xe^s , knowledge of which is essential for measuring LCBF.

We describe methods for graphing PEXe^s saturation and desaturation curves concurrently with serial CT scans of the brain measured in horizontal and coronal planes after brief inhalation of mixtures of 30%–80% Xe^s in oxygen. Forty blood flow measurements were made in 10 normal baboons to determine the accuracy and reliability of the cerebral blood flow measurements. Steady state reproducibility, effects of hypocarbia, hypercarbia, anesthesia, and brief anoxia were all tested. Comparable LCBF measurements in baboons after experimental cerebral embolism and infarction are the subject of a separate report [6].

Materials and Methods

Preparation of Animal Models

Ten baboons (*Papio anubis*) weighing 5–7 kg were used for measurements of LCBF and λ values by inhalation of Xe^s and measurement of cerebral tissue saturation and desaturation by CT scanning with the EMI scanner. Forty satisfactory saturation and desaturation measurements of cerebral clearance of Xe^s recorded concurrently from each of two coronal or horizontal slices of brain tissue, 4 mm apart, were analyzed.

In 14 additional baboons regional cerebral blood flow (rCBF) measurements were made under comparable experimental condi-

tions using the ^{133}Xe intracarotid bolus and inhalation methods for purposes of comparison [22, 23, 26].

Prior to all surgical manipulations, light anesthesia was induced by intramuscular injection of ketamine hydrochloride (Ketalar, 2 mg/kg body weight) supplemented as required by regional injection of 1% lidocaine hydrochloride at all incision and catheterization sites. Tracheostomy was made under sterile conditions, with insertion of a plastic endotracheal tube. Metal fittings were avoided because they are a potential cause of CT artifact. Immediately prior to CT scanning, temporary immobilization was assured by intravenous injection of pancuronium bromide in doses of 0.2 mg/kg and respiration was assisted with a Harvard respirator.

Relevant physiological variables were monitored by using a distortion-free ink-writing polygraph, with linear response and maximum pen deflection of 25 cm. End-tidal partial pressure of carbon dioxide (PECO_2) and oxygen (PEO_2) were recorded by a Godart capnograph (type 146, Instrumentation Associates, New York, NY) and Beckman OM15 oxygen monitor (Beckman Instruments, Fullerton, CA). End-tidal Xe^s was monitored by using a Gow Mac thermoconductivity gas analyzer (Gow Mac Instrument Co., Bound Brook, NJ). Blood pressure was recorded by using a strain gauge connected to a catheter placed in the aorta via the femoral artery.

In two animals, the PEXe^s measured by thermoconductivity was compared to ΔH units of a series of arterial blood samples. Arterial blood samples were drawn for determination of hematocrit and hemoglobin values after each CT study. The electroencephalogram (EEG) was recorded from each hemisphere throughout the Xe^s inhalation in all animals except the two in which coronal sections were made. In these two animals the EEG recordings were omitted because the EEG electrodes interfered with the CT scans.

CT Scanning

An EMI 1010 CT unit was modified with 180 mm wedges, and a 4 mm collimator. The unit was fitted with a cursor for selecting regions of interest assisted by a graphics enhancement device (4S, EMI) which permitted recording ΔH changes with a resolution as small as 0.04 cm^3 ($0.1 \text{ cm}^2 \times 0.4 \text{ cm}$). By ΔH changes, we mean the change in Hounsfield units during saturation and desaturation of brain and blood with Xe^s gas. With our instrument, ΔH values breathing air in the steady state are recorded plus or minus one standard deviation (for either gray matter or for white matter), so that changes induced by xenon inhalation of $\Delta 2 \text{ H}$ or more may be considered reliable. The x-ray beam was adjusted to 100 kVp at 40 mA with a 60 sec scanning mode. Two scans were made 4 mm apart with each 60 sec exposure. Scans of the same region were usually made at 1 min intervals for a series of four scans with a 30 sec pause for computer processing before the next series began.

Seven baboons were placed only in the conventional position for horizontal scans with the head slightly flexed to obtain scan angles of 0.10° above the orbitomeatal line. Two baboons were prepared with the head hyperextended so that the scans were made only in the coronal plane, and in one baboon scans were made in both coronal and horizontal planes. The head was placed in a polystyrene block, thereby centered and immobilized in the CT aperture. The baboon reclined comfortably on the infant couch. To minimize CT artifacts, a plastic endotracheal tube was used for maintaining assisted ventilation during the immobilization necessary for the scanning procedures. The EEG electrodes were placed on the scalp so that they did not encroach in the CT field.

Xenon Inhalation

Pure (100%) commercial xenon was obtained as a custom medical diagnostic device for use with the CT scanner from Union

Carbide Corp. (Linde Division, Houston, TX) in 50 liter tanks. Mixtures of 30%, 35%, 40%, 50%, and 80% Xe^s in oxygen were prepared by filling polyethylene bags of known volume with measured parts of 100% Xe^s and 100% O₂. The resultant mixture to be inhaled was then checked for oxygen and Xe^s content by the gas analyzers. Different time intervals of inhalation of the Xe^s mixture were tested (2, 3, 4, 7, 10, and 20 min) in order to determine optimal inhalation and scanning times for LCBF and λ measurements.

O₂ (100%) was breathed for at least 10 min before Xe^s inhalation in order to desaturate nitrogen from the tissues. Mixtures of 30%–80% Xe^s in oxygen were then substituted for 2–20 min intervals. Since end-tidal Xe^s was monitored as well as PEO₂, preliminary desaturation of nitrogen from the brain and body simplified calculation of Xe^s and oxygen concentrations. Also, brain tissue was saturated with Xe^s more rapidly and efficiently because of Henry's law of partial pressures, whereby the brain tissue PO₂ is higher than capillary PO₂ during Xe^s inhalation, hence Xe^s moves rapidly into brain tissue to displace the oxygen in the absence of nitrogen. At least five scans were made during the washin period at 60–90 sec intervals which were accurately noted on both polygraph and CT scans. Once the Xe^s had equilibrated, as judged by plateaus achieved by both end-tidal gas values and brain CT ΔH units, oxygen inhalation was reinstituted and the next series of CT scans was carried out during the washout period. The PEXe^s and PEO₂ were monitored throughout and showed mirror image patterns of change. Knowledge of either could be used for determining arterial Xe^s levels when calculating blood flow values, although direct measurements of PEXe^s are recommended. Oxygen (100%) is a mild cerebral vasoconstrictor, reducing LCBF values for gray matter by at most 5%–10% and white matter by considerably less. However, during the LCBF measurements, 20%–70% oxygen was inhaled which would have minimal vasoconstrictive effects well within our experimental error of 10%.

After Xe^s cerebral blood flow studies were completed, CT scans were repeated at comparable levels after intravenous injection of 1.2 g iodine/kg body weight in the form of diatrizoate meglumine (Reno-M-DIP, Squibb) to better visualize intracranial anatomy and to aid in accurate definition of regions selected for LCBF measurements.

Neuroanatomic Studies

All brains were removed after sacrifice of the animal and fixed in 10% formalin. After fixation for 1 week, the brains were sectioned in 4 mm slices in the same horizontal or coronal planes in which the CT scans had been made. These were photographed and compared with CT sections used for Xe^s measurements to assure correct selection of regions of interest. Representative blocks were embedded in paraffin, sectioned at 15 μ m and stained with hematoxylin and eosin, Luxol fast blue, phosphotungstic acid hematoxylin, and Gomori trichrome stains.

Results

General Observations

Inhalation of mixtures of 50%–80% Xe^s in oxygen for 2 min or longer produced visible changes in serial CT scans of the brain during saturation and desaturation. When saturation was achieved the entire brain, except the ventricles, had a diffuse and homogenous white appearance (fig. 1) although the ΔH units were higher in white matter than gray matter (fig. 2). The greater solubility of Xe^s in white matter

compared to blood and to gray matter is indicated by the larger ΔH units measured for white matter compared to blood or gray matter during saturation. When 50% Xe^s was inhaled, the ΔH units were proportionately reduced by about five-eighths of that seen during 80% Xe^s inhalation (fig. 2). When other mixtures of Xe^s were inhaled (such as 30%) they likewise showed linear relationships to the concentration of Xe^s in the inspired air. Reliable λ values were determined with inhalation of Xe^s mixtures as low as 27%; however, for LCBF measurements, mixtures of at least 35%–40% Xe^s are recommended in order to insure that the ΔH units are sufficient to provide reliable data for calculation. In humans, the ability to measure larger volumes of homogeneous tissue should permit LCBF measurements with sub-anesthetic concentrations of Xe^s and improved counting statistics. During saturation, gray matter showed more rapid increases in tissue density and ΔH units than white matter, reflecting the more rapid rate of perfusion of gray matter. Likewise, during desaturation, gray matter cleared more rapidly due to its higher rate of perfusion, leaving the white matter with its slower rate of perfusion and its great solubility for Xe^s temporarily in relief (fig. 1). During saturation with Xe^s, all the ventricles were clearly outlined, since there was no apparent entry of Xe^s into the cerebrospinal fluid (fig. 1). The pattern of change during desaturation was the reverse of that seen during saturation.

In Vivo Determination of Tissue-Blood Partition Coefficients

Brain-blood partition coefficients (λ) for all regions of interest were obtained using the following formula:

$$\lambda = \frac{\Theta \text{Xe}^s (\text{tissue})}{\Theta \text{Xe}^s (\text{blood})} \quad (1)$$

where ΘXe^s are the relevant tissue solubilities for Xe^s between brain and blood. Satisfactory data was obtained by inhalation of 30% Xe^s until saturation was achieved. Anesthetic effects are avoided by the use of low concentrations. To obtain blood or brain tissue Θ values with the CT scanner, the ΔH values for different regions of brain tissue are measured at saturation from the following equation [10]:

$$\Theta \text{Xe}^s = \Delta H \times \frac{\mu_p^w / \mu_p^{\text{Xe}^s} \times 100}{5.15 \times C} \quad (2)$$

where ΔH is the increase in Hounsfield units (H) at saturation with Xe^s in both arterial blood and brain regions of interest; μ_p^w is the mass attenuation coefficient for water; $\mu_p^{\text{Xe}^s}$ is the mass attenuation coefficient for Xe^s. Xe^s gas density under ideal conditions is 5.15 mg/cm³ at 760 mm Hg and at 37°C. This value was used in solving equation 2. C is the percentage concentration of Xe^s inhaled. Ratio ($\mu_p^w / \mu_p^{\text{Xe}^s}$) varies with the kilovoltage used and must be determined empirically for each CT scanner setting.

Two methods were used for calculating λ :

1. *Direct determination of λ in vivo.* Brain tissue saturation after inhalation of Xe^s was assumed when plateaus appeared in both arterial and brain ΔH values. In practice this was consistently seen within 10 min of the start of inhalation

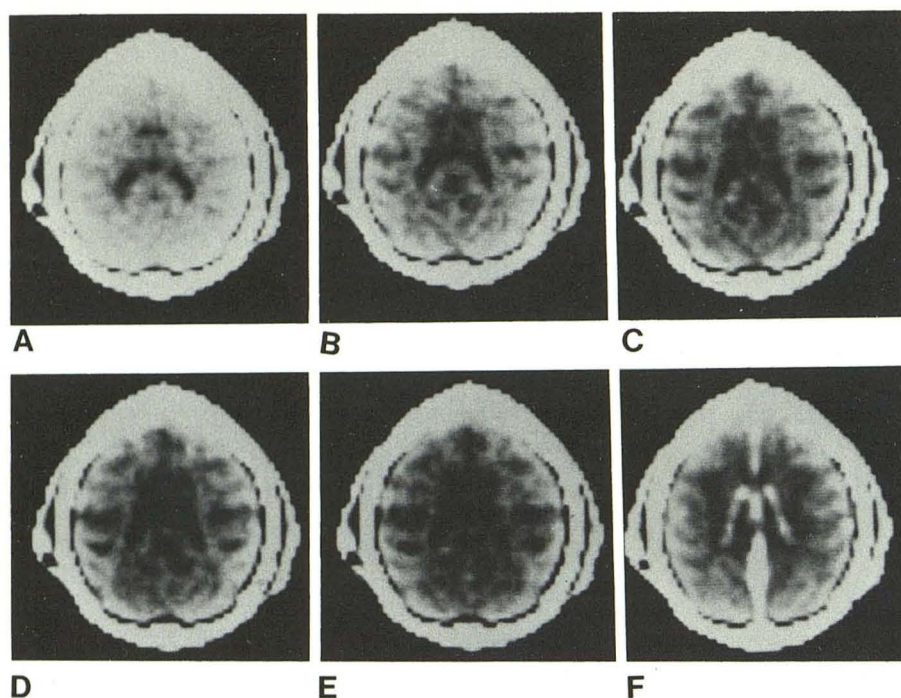


Fig. 1.—Normal Xe^s desaturation of entire brain slice by serial CT scans. A, 1 min scan made at saturation 10 min after starting Xe^s inhalation. Homogeneous Xe^s enhancement of entire brain except for lateral ventricles. B–E, Serial 1 min scans made after initiation of 100% oxygen inhalation. Rapid clearance of Xe^s contrast from cortical gray matter which creates temporary enhancement of white matter (in D). F, Iodine contrast scan made after completion of Xe^s scans, at same level. Cortex choroid plexus, and falx cerebri are seen. For LCBF measurements, regions of interest are selected and ΔH units recorded from those regions.

(fig. 2). If λ values were determined before tissue saturation was complete, they tended to be underestimated. (Curves could be extrapolated to plateaus, however, thereby avoiding underestimation.) Arterial blood samples were drawn at corresponding time intervals in plastic syringes and scanned in a plastic phantom in the same manner as the brain tissue. Thus the ΔH units for both artery and brain tissue were obtained and λ could be calculated directly by substitution of ΔH in the following equation:

$$\lambda = \frac{\Delta H (\text{tissue})}{\Delta H (\text{arterial blood})} \quad (3)$$

2. Indirect determination of the solubility of Xe^s in blood Θ of different hematocrits. The solubility of Xe^s in blood is related to the hematocrit value (Ht) which may be expressed by the following formula [26]:

$$\Theta \text{Xe}^s \text{ blood} = 0.0011 \times \text{Ht} \left(\% \frac{\text{vol RBC}}{\text{vol Blood}} \right) + 0.10 \quad (4)$$

Thus $\Theta \text{Xe}^s \text{ blood}$ may be substituted for the denominator of equation 1. However, calculation of the $\Theta \text{Xe}^s (\text{tissue})$, which is the numerator of equation 1, using equation 2 requires knowledge of $\mu_p^w / \mu_p^{\text{Xe}^s}$ which was measured in vivo—equation 2 may be rewritten:

$$\mu_p^w / \mu_p^{\text{Xe}^s} = \frac{\Theta \text{Xe}^s \times 5.15 \times C}{\Delta H \times 100} \quad (5)$$

The blood of known hematocrit for the baboon was scanned before and after saturation with a known concentration of Xe^s (C) and the ΔH obtained. $\Theta \text{Xe}^s (\text{blood})$ was calculated separately using equation 4. In three baboons ($\mu_p^w / \mu_p^{\text{Xe}^s}$) was calculated using the CT scanner with the kilovoltage set at 100 and was found to be $2.54 \times 10^{-2} \pm$

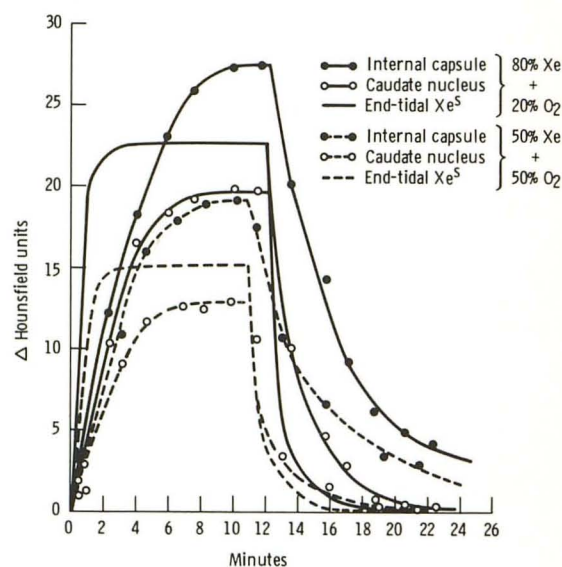


Fig. 2.—Saturation and desaturation curves during inhalation of mixtures of 50% and 80% Xe^s in oxygen in normal baboon for intervals of 11 and 12 min. Typical end-tidal, internal capsule, and caudate clearances are shown; clearances of numerous other regions of brain were concurrently measured.

0.4×10^{-2} . Thus, ΔH for blood at saturation, may be calculated from equation 5 and knowledge of the percentage concentration (C) of the xenon mixture. If the change in end-tidal Xe^s (PEXe^s) values measured by the thermoconductivity sensor are now multiplied by this result, the PEXe^s values are then expressed in ΔH units. Indirect calculation for λ (partition coefficient or solubility between blood:brain) may now be achieved using this constant without having to obtain ΔH for each arterial sample. In practice to render the method noninvasive, the ΔH changes for arterial blood were

estimated at 10 sec intervals from the percentage change in thermoconductivity values for PEXe^s (which is in equilibrium with arterial blood) and after conversion to equivalent ΔH values, may then be substituted as the arterial blood values when calculating LCBF values. For example, when 100% oxygen was breathed, PEXe^s was assumed to be zero; when saturation was achieved this value was assigned 100%. Percentage PEXe^s values were then multiplied by the ΔH values for blood at saturation determined directly by scanning arterial or venous blood samples or indirectly by using equation 5 and knowledge of the hematocrit.

End-tidal Xe^s concentration was monitored by the use of a Gow-Mac thermoconductivity gas analyzer. This instrument showed a linear response for detecting Xe^s using calibrating mixtures of known content obtained commercially with an error of less than -5% for Xe^s versus 100% oxygen and +3% for 100% nitrogen (fig. 3). There was no distortion due to changes in PECO₂ or H₂O vapour within the physiological range.

The end-tidal Xe^s curve was recorded on the polygraph from the thermoconductivity gas analyzer and was compared with simultaneous recordings and equalized calibrations by use of (1) end-tidal ¹³³Xe mixed with Xe^s recorded by a NaI crystal scintillation detector [26] and (2) from ΔH units obtained by scanning serial arterial blood samples drawn with each scan (fig. 4).

Calculation of Local Cerebral Blood Flow

The theoretical basis for calculation of LCBF using inhalation of Xe^s and CT scanning is derived from the Fick principle. The following equation was reviewed in detail by Kety and Schmidt [27, 28]:

$$Cb(T) = \lambda K_1 \int_0^T Ca(t) e^{-K_1(T-t)} dt \quad (6)$$

where $Cb(T)$ is the concentration of the tracer substance (Xe^s) in the brain region of interest at a given time T_1 ; λ is the tissue-blood partition coefficient for the tracer substance; K_1 is the rate of blood flow per unit of tissue volume (fi) divided by λ ; and $Ca(t)$ is the changing concentration of Xe^s in the arterial blood or end-tidal air (with which the arterial gas is in equilibrium) during the time interval $0-T$.

In order to calculate the blood flow to a given region of the brain the following variables were measured: (1) concentrations of Xe^s in the brain tissue regions of interest; (2) the time course of changes in the arterial blood or end-tidal concentration of the tracer, Xe^s; and (3) tissue-blood partition coefficient (λ) for the given region of the brain.

The following five different methods for calculation K_1 values with or without deconvolution were attempted:

1. The biexponential model of Obrist et al. [22] provided an algorithm for computer solution of both K_1 (fast clearance) and K_2 (slow clearance). This was found to be applicable when selected brain regions of interest were large and included both gray and white matter so that a biexponential clearance of Xe^s resulted. The changes in ΔH units for end-tidal PEXe^s at 10 sec intervals were used for the

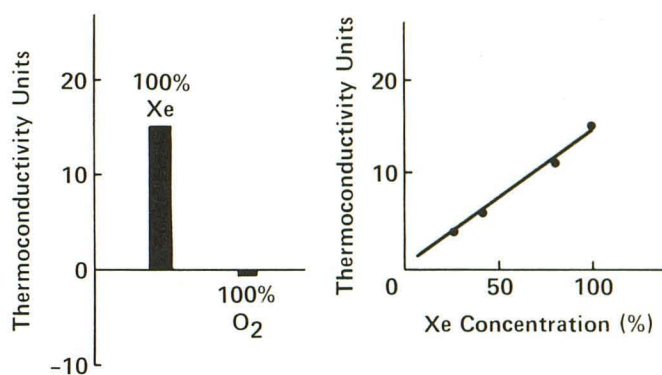


Fig. 3.—Calibration of Gow Mac thermoconductivity gas analyzer. Left panel shows response of meter to 100% Xe^s compared to 100% oxygen. Small oxygen response is in opposite direction (error less than -5%). On right is plot of series of four calibrating gas mixtures; response of meter is linear. Testing was also carried out with H₂O, nitrogen, and CO₂ in their physiological ranges; all indicated nitrogen errors less than +5%.

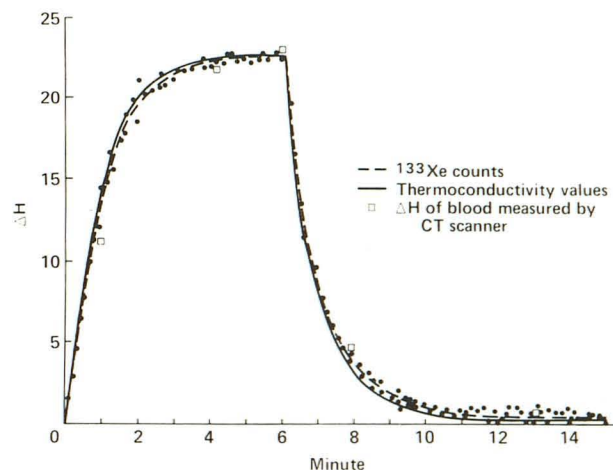


Fig. 4.—Normalized, superimposed plots of arterial Xe^s content during inhalation of 80% Xe^s for 6 min, graphed as: ΔH units of samples of arterial blood measured by the CT scanner (open squares), end-tidal ¹³³Xe label (broken line and dots), and thermoconductivity values measured in end-tidal air (solid line). All methods of measurement are in good agreement.

“air curve” plus the ΔH units determined from 7–10 serial CT scans of the brain where large regions of interest were selected for computer analysis. The program of Obrist et al. was used with a PDP 1105 microprocessor [26].*

2. A monoexponential model was programmed for the DEC 10 computer. This is a modification of the model of Obrist et al. [22] using single compartmental analysis. This provided solution for K_1 when the selected brain region of interest was sufficiently small to provide homogenous flow. This was confirmed by visual inspection of the monoexponential appearance of the clearance curves and calculation of λ values typical for pure gray or white matter.*

* See NAPS Document no. 03640 for 11 pages of explanatory notes. Order from ASIS/NAPS, c/o Microfiche Publications, P.O. Box 3513, Grand Central Station, New York, NY 10017. Remit in advance, in US funds only, \$5.00 for photocopies or \$3.00 for microfiche. Outside the US and Canada, add postage of \$3.00 for photocopy and \$1.00 for microfiche.

3. An algorithm was specially programmed for the DEC 10 computer using an in vivo autoradiographic analysis.* The principle is based on equation 6 of Kety and Schmidt [27, 28], but is derived from the early models of Landau et al. [29] and Reivich et al. [30] determined by postmortem autoradiographic analysis. The arterial saturation values in ΔH units were calculated at 10 sec intervals from the PEXe^s curves. This proved to be ideal when the selected regions of interest were sufficiently small so that homogeneous tissues of either gray or white matter were measured. (It should be emphasized that using methods 2, 3, and 4, it is essential that small, homogeneous regions of tissue are selected.) Theoretical considerations for application of this model in vivo to emission tomography have been discussed by Kanno and Lassen [24]. In this model, knowledge of the concentration of Xe^s in the brain at any point in time (T) measured during saturation was provided by 1 min scans together with knowledge of the arterial saturation curves provided by PEXe^s measurements. With the EMI scanner serial measurements of LCBF were measured at intervals of 1 min. Ability to measure LCBF from a single 1 min scan during Xe^s inhalation is a distinct advantage, since the head need only be held still for 3–4 min and with newer scanners, scanning intervals of a few seconds may be possible.

4. The original formula for CBF measurement first described for the nitrous oxide technique by Kety and Schmidt [28] was modified. The ΔH curves from small regions of interest and recorded from serial scans were used to provide tissue saturation and desaturation curves considered to be in equilibrium with capillary venous blood. The arterial (end-tidal) clearance curves and tissue clearance curves were normalized and plotted as a graph defining the areas between the two curves. This method calculates regional 10 min flow values but it is time consuming, impractical, and with 80% Xe^s low values due to its anesthetic effects are apparent.

5. The method proposed by Pasztor et al. [31], where the $T\ 1/2$ of each desaturation curve in the region of interest was determined from the semilogarithmic plot after ignoring the first 40 sec where recirculation is maximal, was modified. This did not give reliable absolute quantitative flow values, because there was incomplete correction for recirculation. It was used as a relative index of flow and was compared to the other methods.

Typical results are illustrated in tables 1 and 2 for LCBF calculated by methods 2–5. Results using the bicompartamental method will be briefly described. Compared to the in vivo autoradiographic method which is considered best, the biexponential method of Obrist et al. [22] gave lower values for white matter flow, comparable values for gray matter flows, but was less localized and reliable since the λ s of gray and white matter were not accurately measured, and presumptive flows of gray and white matter (F_1F_2) are arbitrarily assigned to the slow and fast clearing compartments in this model.

The monoexponential method of Obrist et al. [22] gave similar values for the same regions examined as the in vivo autoradiographic method, but took longer to calculate, did not provide minute-to-minute flow values, was less accurate

during brief inhalation intervals, required immobilization of the head for 10 min, and arbitrarily assigned all low flows to white matter. All LCBF values measured after 10 min of 80% Xe^s inhalation showed reduction due to anesthetic effects at this high concentration. Anesthetic effects on LCBF were not seen with Xe^s mixtures below 50%.

Determination of Cb(T) by CT Scans

Method 3, termed the in vivo autoradiographic method, proved best and most practical for several reasons. The ΔH units for each region of interest during saturation for each of two brain sections recorded concurrently 4 mm apart were measured by examining volumes as small as 0.04 cm^3 (4 voxels). At 1 min intervals the Hounsfield units were reproducible with low standard deviations, and computed LCBF values showed statistically significant reproducibility. Thus, minute-to-minute flow values were obtained. Once λ is obtained by a saturation scan after inhalation of 30% Xe^s for 10 min, inhalation of greater concentrations may be inhaled briefly so that immobilization of the head for only 3 min is necessary to obtain reliable flow data if autoradiographic analysis is used.

Autoradiographic analysis is only programmed for LCBF measurements during saturation. However, the graphics enhancement software may be used to select regions of interest of any desired shape and anatomic locus. Mono- or biexponential algorithms may also be used to calculate LCBF data recorded from the same two brain sections during each saturation and desaturation interval so that, once the data are recorded, handling is flexible and different methods of analysis may be used to confirm any LCBF values that may appear unusual.

During different inhalations and in different normal baboons, reliable LCBF measurements were collected throughout representative regions of both hemispheres and brainstem–cerebellar regions (tables 2 and 3). Horizontal sections offer the greatest volume of brain tissue for LCBF measurements. Coronal sections have the advantage of better discrimination for certain anatomical loci such as the temporal lobes, insular regions, hippocampus, internal capsule, and the brainstem. Serial LCBF measurements were highly reproducible (fig. 5) ($r = 0.89$, $p < 0.05$). The measurement error (coefficient of variation) was 5.2% for λ values and 10.2% for LCBF values, which compare favorably for hemispheric values measured in the baboon with the ^{133}Xe method [32] and rCBF values measured with ^{133}Xe method in man (table 4) [22, 23]. Absolute values for gray matter were in excellent agreement with ^{133}Xe values (table 5). White matter flow values determined by the in vivo autoradiographic or monoexponential methods were consistently higher. Possible explanations for this will be discussed later.

Estimated Methodologic Error in Determining Tissue Clearance Curves for Xe^s by CT Scanning

Potential distortions of brain tissue saturation and desaturation curves plotted from ΔH units derived from serial 60

TABLE 1: 80% Xe^s Measurements of Partition Coefficients and Local Cerebral Blood Flow Values Compared by Different Methods of Computation in the Unanesthetized Baboon

Brain Matter	Partition Coefficient (λ)	LCBF (ml/100 g brain/min)				
		In Vivo Autoradiographic Analysis	Monoexponential Analysis		T 1/2 Analysis, 10 min Inhalation	Kety-Schmidt Modification, 10 min Inhalation (mean flow)
			3 min Inhalation	10 min Inhalation		
Gray (caudate nucleus)	0.88	91	99	57*	25*†	45*
White (internal capsule)	1.25	37	43	42*	24*†	

Note.—Data on one baboon.

* Reduced by anesthetic effect.

† Uncorrected for recirculation.

TABLE 2: Regional Cerebral Blood Flow in Normal Baboons by Inhalation of 80% Xe^s in Oxygen

Region	Partition Coefficient (λ)	CBF (ml/100 g brain/min)		
		Monoexponential Analysis		Autoradiographic Analysis at 1–2 min
		1.5–3 min Inhalation Interval	10 min Inhalation Interval	
Cortex:				
Frontal	0.99	90.2	47.4	76.9
Postcentral	0.97	74.0	56.0	68.4
Occipital	1.06	106.0	59.0	86.7
Posterior parietal	1.04	103.0	86.1	99.0
Cerebellar	0.99	72.6	65.4	75.7
White:				
Frontal	1.22	45.0	25.8	42.0
Occipital	1.23	50.3	25.9	46.7
Cerebellar	1.25	44.2	31.6	50.6
Vermis	1.02	64.3	61.5	53.6
Lenticular nucleus	1.01	105.0	73.6	97.0
Caudate nucleus	0.91	98.7	52.8	80.6
Internal capsule	1.25	43.8	40.2	42.8
Colliculi:				
Inferior	1.18	143.0	99.0	118.0
Superior*	1.20	93.4	84.0	90.3

Note.—Data on two baboons.

* Midbrain at level of superior colliculi.

sec CT scans were estimated by comparing them with theoretically synthesized curves of known K values (fig. 6). The theoretical curves were constructed by convolution from the actually measured arterial input using a theoretical monoexponential cerebral function according to the equation of Kety and Schmidt [28]. Figure 6 illustrates an example of theoretically synthesized brain tissue ΔH curves derived from the actually measured arterial ΔH curves during inhalation of 80% Xe^s in oxygen by use of their formula assuming $K = 1$ and $\lambda = 1$.

The solid line in figure 6 represents the smoothed theoretical monoexponential curve for brain tissue derived from the known K values for the given arterial input. The area of each bar is the integral of the curve during each 60 sec time interval. Superimposition of actual measured ΔH curves for brain tissue derived by plotting midpoints of peak ΔH units measured by this CT scanner at 1 min intervals gave values similar to the predicted curve. The value for K obtained from the measured curves of ΔH units gave agreement within 2%–5% when compared to the synthesized curves.

Comparison of LCBF Values Calculated by Different Methods

LCBF values calculated for the same regions of brain by monoexponential, in vivo autoradiographic, T 1/2, and Kety-Schmidt 10 min modified methods for computation by CT scanning were in good agreement except for predictably low values by the T 1/2 method of analysis since there was no correction for recirculation (tables 1–3). (Calculations from the two-compartmental model will be discussed later.) LCBF values derived from 80% Xe^s clearance in which saturation was continued for 4 min or longer showed a progressive decline (tables 1 and 2, fig. 7). This was due to the anesthetic effects of high concentrations of Xe^s since the EEG showed progressive slowing after 3–4 min (fig. 8) and the decline was not seen if 30%–50% Xe^s was used or inhalation was brief. In other words, anesthetic effects are avoided by limiting the inhalation interval of 80% Xe^s to 3 min or the use of concentrations between 30%–50% Xe^s.

In vivo autoradiographic or monoexponential measure-

TABLE 3: Local Cerebral Blood Flow and Partition Coefficients Measured by the In Vivo Autoradiographic Method After Xe^s Inhalation in Normal Awake Baboons

Region	Partition Coefficient (λ) \pm SD	Blood Flow (ml/100 g brain/min) \pm SD
Cortex:		
Cerebellar	0.96 \pm 0.08	78.0 \pm 15.7
Occipital	0.94 \pm 0.08	78.9 \pm 9.2
Parietal	0.93 \pm 0.08	73.9 \pm 11.7
Frontal	0.96 \pm 0.08	76.9 \pm 2.4
Thalamus	0.98 \pm 0.11	91.2 \pm 5.9
Caudate	0.90 \pm 0.08	79.0 \pm 12.3
Colliculi:		
Inferior	1.18 \pm 0.05	132.0 \pm 20.0
Superior*	1.08 \pm 0.16	94.2 \pm 7.9
Vermis	0.97 \pm 0.01	76.5 \pm 21.5
Internal capsule	1.29 \pm 0.03	52.3 \pm 8.3
White matter (centrum semiovale)	1.29 \pm 0.03	36.4 \pm 3.7

Note.—Data from eight baboons.

* Midbrain at level of superior colliculi.

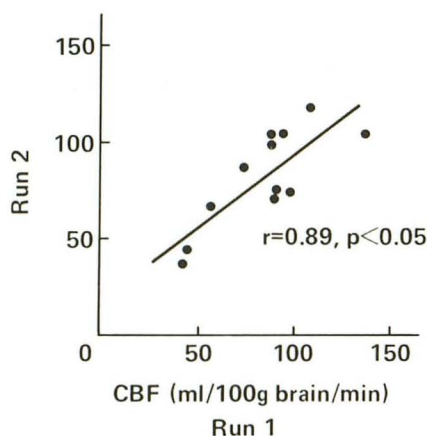


Fig. 5.—Reproducibility of in vivo autoradiographic method for concurrent measurements of LCBF of 12 regions of brain in unanesthetized baboon repeated at 30 min intervals. Similar reproducibility was confirmed in other animals.

ments for white matter gave somewhat higher flow values of 36.4–52.3 ml/100 g brain/min for the baboon compared with values measured by the ¹³³Xe inhalation method. These higher white matter flows may be due to a number of factors, such as exclusion of scalp and extracerebral contamination and the earlier estimation of flow with the first 2–3 min of arrival of the indicator. It should be borne in mind that conventional estimates of white matter flow from two-compartmental analysis assume that low flows are all of white matter origin. Measurements in one of our baboons (but not tabulated here) using both two-compartmental analysis of larger regions of the midbrain compared to multiple smaller volumes of the same regions measured by the in vivo autoradiographic technique showed considerably lower values measured by two-compartmental analysis for “white matter” of 27–41 ml/100 g brain/min while gray matter flows

for the colliculi were similar, being 143–152 ml/100 g brain/min. Likewise, if ΔH changes for larger regions of the hemispheres were recorded in the same animal and LCBF of hemispheric white matter were calculated by the biexponential algorithm and the use of traditional λ values of 1.5 [26], white matter flow values were 25–30 ml/100 g brain/min in the baboon.

Highest gray matter flow values were measured in regions of the inferior colliculi. Mean hemispheric LCBF values for gray matter were in good agreement with ¹³³Xe measurements of hemispheric blood flow in the unanesthetized baboon (table 5) [26]. They are also consonant with independent estimates of LCBF in the baboon made by Drayer et al. [1] under light barbiturate anesthesia after Xe^s inhalation and serial CT scanning of Xe^s clearance from arterial blood and brain. Local CBF measurements reported here and calculated by Xe^s in vivo autoradiography show good correlation with measurements of local glucose consumption in the monkey measured by the deoxyglucose method and postmortem autoradiography [32]. This is to be expected from the well known cerebral blood flow–metabolic couple present in normal brain. Regional differences in gray matter flow values were similar to those reported in the cat by Landau et al. [29] and Reivich et al. [30] using postmortem autoradiographic methods.

In vivo calculations of λ values (tables 1–4) were the same whether measured with 27% or higher Xe^s concentrations; therefore, they may be determined with prolonged inhalation of safe and nonanesthetic Xe^s mixture. The λ values for gray matter were 0.88–1.18 (mean, 0.92); λ values for white matter were 1.22–1.25 (mean, 1.24). Mean values for mixtures of gray and white matter were 1.12 which agree well with mean values determined for dead human brain [20]. The overall measurement error for normal λ values is 5.2 \pm 1.9%, which should be useful in future estimations of pathologic changes in tissue composition due to brain edema [6].

The time required for calculation of 15 LCBF values, using the in vivo autoradiographic method and our computer program (including accession of data points from end-tidal air and 15 brain tissue curves), is 20 min. Solution for each LCBF value by computer takes 10 sec.

Optimum scanning time determined from serial 1 min flow estimates, after 80% Xe^s inhalation, is 1–3 min (fig. 7). During the first 30 sec, there is insufficient saturation of brain and blood for reliable measurements. After 3 min the anesthetic effects of 80% Xe^s decrease LCBF values. If lower, subanesthetic concentrations are inhaled, all values are highly reproducible without anesthetic effects. Concentrations of 35%–45% Xe^s in oxygen are ideal to avoid anesthetic effects. Multiple concurrent measurements of LCBF after 2 min inhalation show statistically significant reproducibility when repeated 30 min later (fig. 5).

Effects of Hypocapnia and Hypercarbia on LCBF

Decreasing the PE_{CO}₂ by hyperventilation decreased LCBF of both gray and white matter diffusely and homogeneously throughout the brain (fig. 9). There was no particular

TABLE 4: Measurement Error Between First and Second Measurements in Awake Baboons

	Mean (\bar{x})	SD	SD/ \bar{x} (%)	Mean
Partition coefficient (λ):				
Thalamus	1.03	0.08	7.8	5.2 \pm 1.9
Caudate	.87	.05	5.7	
Internal capsule	1.24	.02	1.6	
Lenticular nucleus	.97	.05	5.2	
Cortex:				
Frontal	.92	.04	4.3	5.2 \pm 1.9
Parietal	.89	.06	6.7	
Occipital	.90	.05	5.6	
Local blood flow:				
Thalamus	96.1	4.2	4.4	10.2 \pm 4.1
Caudate	85.7	11.4	13.3	
Internal capsule	50.6	6.5	12.8	
Lenticular nucleus	97.0	6.7	6.9	
Cortex:				
Frontal	76.9	6.1	7.9	10.2 \pm 4.1
Parietal	71.5	7.2	10.1	
Occipital	80.2	13.0	16.2	

Note.—Data on two baboons.

TABLE 5: Comparative Mean Hemispheric Blood Flow Values Measured by ^{133}Xe and Xe^s Inhalation

	Flow During Awake State (ml/100 g brain/min)		Flow During Anesthesia (ml/100 g brain/min)	
	Fg	Fw	Fg	Fw
^{133}Xe inhalation (biexponential analysis)	84.1 \pm 8.6	25.8 \pm 2.1	52.7 \pm 2.5	23.7 \pm 3.4*
Xe^s inhalation (in vivo autoradiographic analysis):				
0.5–2.5 min	82.3 \pm 8.3	40.3 \pm 8.2	52.1 \pm 7.9	32.0 \pm 1.9*
6–7 min	45.0 \pm 6.3	27.8 \pm 3.0†

Note.—Fg = flow, gray matter; Fw = flow, white matter. Hemispheric blood flow values during Xe^s inhalation were calculated by averaging Fg values for frontal, parietal, occipital, caudate nucleus, thalamus, and lenticular nuclear gray matter; and Fw values for frontal, parietal, occipital, and internal capsule.

* Sodium pentobarbital, 5 mg/kg intramuscularly.

† 80% Xe^s .

region which showed excessive reduction. Likewise, hypercarbia caused a homogenous increase of CBF throughout the brain, all regions showing comparable cerebral vasomotor responsiveness. For example, LCBF values of the gray matter of the cerebral hemispheres, cerebellum, and brainstem showed similar cerebral vasomotor responsiveness ($\Delta\%$ CBF/ $\Delta\text{mm PEco}_2$) of circa 3.0% which is similar to that seen in man [33] and previously reported in the baboon by the ^{133}Xe method [26].

Effects of Anesthesia

Light pentobarbital anesthesia (sodium pentobarbital, 5–10 mg/kg body weight intramuscularly) or 80% inhalation of Xe^s for 7 min caused a reduction of LCBF of cortical and subcortical gray matter and to a lesser extent white matter (fig. 10, table 5). The reduction of flow in cerebral gray matter induced by light barbiturate anesthesia was about 30%–50% and similar gray matter reductions were seen during prolonged 80% Xe^s inhalation.

Effects of Anoxia

Brief anoxic anoxia by reducing the oxygen in the inspired air to zero for 3 min caused suppression of all EEG activity and produced a diffuse increase of LCBF values in the order of 20%–30% in both gray and white matter (fig. 11).

Discussion

Advantages of LCBF Measurements by CT Scanning After Xe^s Inhalation

Measurements of LCBF made in vivo by stable xenon (Xe^s) inhalation and CT scanning are noninvasive and have better 3-dimensional resolution than any other methods of measurement of cerebral blood flow currently available. Problems of tissue overlap and Compton scatter are minimized or avoided, and anatomic boundaries of zones of zero perfusion, low flow, or different solubility for Xe^s (such as the ventricles and white matter) are well defined. By activation procedures such as CO_2 inhalation or administration

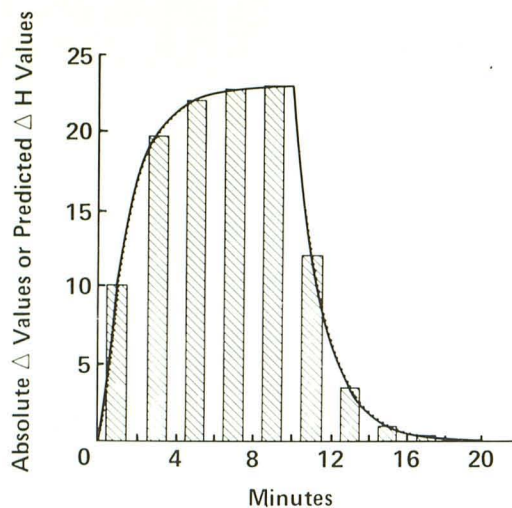


Fig. 6.—Predicted synthetic brain tissue curves (solid line) during saturation and desaturation plotted after convolution from actual arterial Xe^s curves (measured in baboon during saturation and desaturation) using Kety's equation assuming $K = 1$ and $\lambda = 1$ [27, 28, 33]. The cross hatched bars represent actual ΔH unit counts. Area of each bar is integral of curve during each 1 min interval. Predicted and measured curves superimpose well with errors of 2%–5% depending on K values.

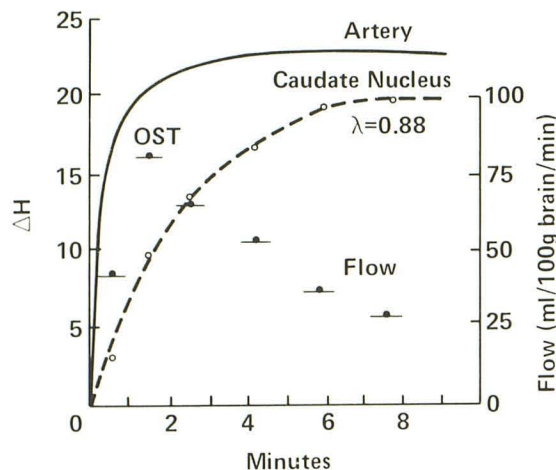


Fig. 7.—Determination of optimal scanning time (OST) estimated from serial in vivo autoradiographic measurements of ΔH values from 1 min scans of caudate nucleus during 80% xenon inhalation. Measurements made between the first and second minutes are optimal. Unless 30%–50% xenon in oxygen concentrates are inhaled, anesthetic effects of xenon lower LCBF measurements. Measurements made within first minute are less reliable, as arterial blood and tissue ΔH values are both rapidly changing and are subject to variations due to circulatory time and respiratory variations.

of pharmacologic agents, CT measurements of LCBF show large and rapid changes occurring within 1 min. The stable xenon CT method overcomes certain limitations of the ^{133}Xe inhalation technique, where zones of zero flow cannot be measured, and Compton scatter and overlap limit resolution [21–23, 26]. With currently available CT scanners having slow scanning time, serial LCBF measurements may be made at 1 min intervals during both saturation and desaturation.

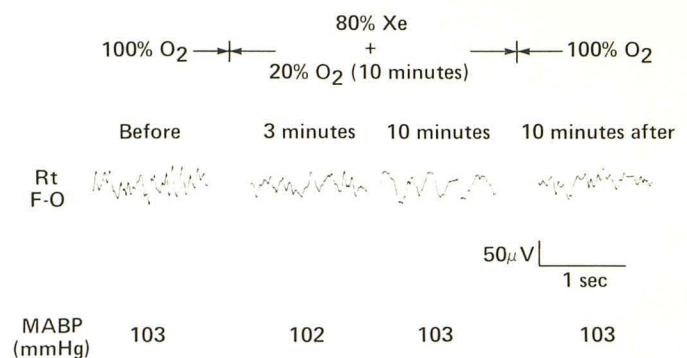


Fig. 8.—Electroencephalogram recorded at different time intervals during 80% stable xenon inhalation in baboon shows anesthetic effects after 3 min as measured in fig. 7.

After inhalation of Xe^s , the relative solubility of tissues (λ) are measured with precision and changes in tissue solubility resulting from disease are quantifiable. Normal anatomic landmarks, such as white matter and gray matter, are better visualized and the regional flow values of all parts of the brain, including the brainstem nuclei, cerebellum, and basal ganglia, may be determined in 3 dimensions with a temporal and spatial resolution hitherto unavailable. CT scanning equipment is widely available and the method should be clinically useful.

Disadvantages of LCBF Measurements by CT Scanning After Xe^s Inhalation

CT scanning with Xe^s inhalation requires serial scans and potentially increases radiation exposure to the eyes, brain, and scalp. By proper positioning of the head, direct exposure to the cornea and lens of the eye is avoided. With the present EMI equipment, each 1 min exposure (measured with an Alderson-Rando head phantom and thermoluminescent dosimeter chips) delivered 1 rad (0.01 Gy) to the center of the brain and 2 rad (0.02 Gy) to the scalp. A series of 15 LCBF measurements gives radiation exposure comparable to that occurring during standard serial cerebral angiography.

Pure 100% stable xenon gas is commercially expensive: the cost for 50 liters is \$385. However, by (1) careful conservation of Xe^s using inhalation intervals of 2–3 min; (2) conservation using mixtures of 40%–50% xenon for LCBF measurements delivered by a closed, rebreathing circuit; and (3) determining λ values by inhalation of 30% xenon for 7 min, the cost of a series of CBF measurements can be reduced to \$100, and the cost of a single LCBF measurement to about \$20, which seems reasonable and practical.

Xenon is anesthetic in high concentrations, and this must be taken into consideration whenever it is used. Although, with present knowledge, metabolism cannot be measured by the CT scanner, Xe^s LCBF measurements may be followed by the intravenous infusion of iodine contrast material [6] for measuring damage to the blood-brain barrier, thereby adding considerably to the dynamic and diagnostic capabilities of the CT scanner.

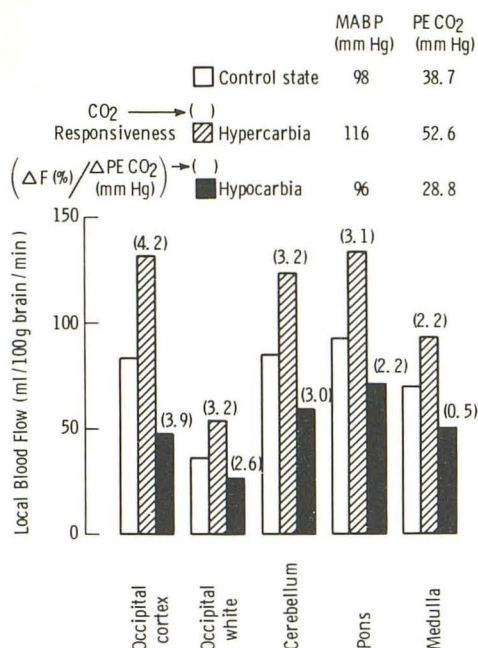


Fig. 9.—Effects of hypercarbia and hypocarbia on local cerebral blood flow of occipital cortex, occipital white matter, cerebellum, pons, and medulla in normal alert baboon.

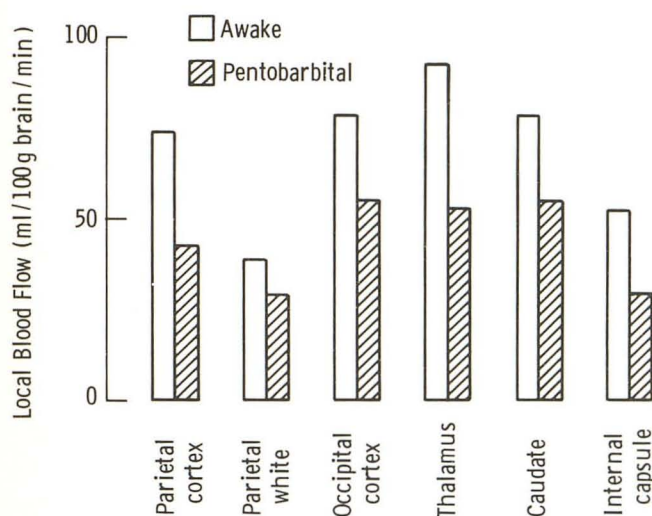


Fig. 10.—Effects of sodium pentobarbital anesthesia administered by intramuscular injection of 5 mg/kg body weight on local blood flow of parietal cortex and white matter, occipital cortex, thalamus, caudate, and internal capsule in healthy baboon.

Validity of LCBF Measurements Made by CT Scanning and Xe^s Clearance

In vivo measurements of LCBF determined from noninvasive measurements of end-tidal Xe^s and CT scanning of cerebral perfusion are in good agreement with previous invasive measurements using CT scanning of brain tissue and arterial blood samples in the baboon [1, 2] and the ¹³³Xe carotid bolus injection method [26]. Because end-tidal

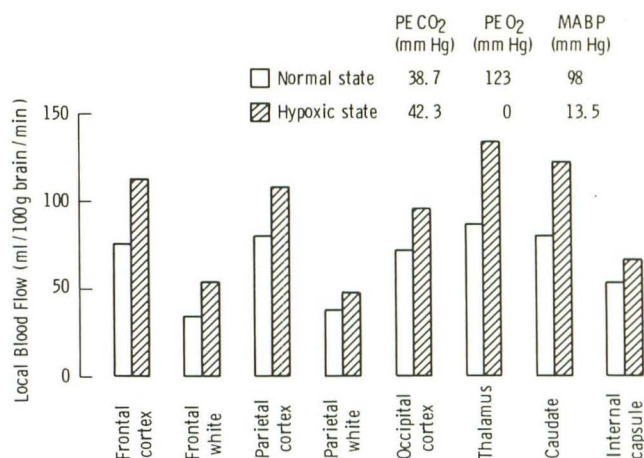


Fig. 11.—Effects of brief hypoxic hypoxia on local cerebral blood flow of frontal and parietal cortex and white matter, occipital cortex, thalamus, caudate, and internal capsule in healthy alert baboon.

curves are continuously recorded, reproducibility and accuracy of the measurements are improved. Indirect evidence of the validity of the measurements is provided by excellent correlation with reported values by local cerebral glucose metabolism measured in the monkey by postmortem autoradiographic techniques [32]. Brain maps of LCBF are now reported in the living monkey, using an in vivo adaptation of the postmortem autoradiographic method, developed in the cat with comparable results [29, 30]. Highest flows are recorded in alert, awake baboons in the vicinity of inferior colliculi, comparable to zones of highest local cerebral glucose metabolism measured in the monkey by postmortem autoradiography [32]. Measurements of LCBF in vivo showed similar effects of anesthesia in reducing cerebral blood flow, particularly in gray matter, as reported previously by postmortem autoradiography in the cat [29, 30]. In our experiments, progressive reductions of LCBF from minute to minute, during induction of anesthesia, correlated with progressive slowing in the EEG.

Hypocapnia and hypercarbia produced expected increases and decreases in CBF. These changes in LCBF were greater in gray matter than in white matter, but were diffusely symmetrical throughout the entire brain, including the brainstem and cerebellar regions consonant with earlier reports [26, 33]. Brief cerebral anoxia produced diffuse increases in LCBF, which is a well known consequence of hypoxic hypoxia.

Technical Considerations Concerning Spatial Resolution, Scanning Speed, and Instability of Attenuation Coefficients

With the modifications of the EMI 1010 scanner described in this study, resolution was sufficient with Xe^s inhalation combined with iodine contrast infusion to differentiate LCBF values for cerebral cortex, white matter, cerebellum and brainstem, and the superior and inferior colliculi. The ventricles showed no change in ΔH units, confirming the resolving power of the method.

It was possible, at counting intervals of 1 min, to record reliable and statistically reproducible changes in ΔH units during and after Xe^s inhalation by measuring regions as small as 0.04 cm^3 . This is estimated to be recording from about 4 voxels of the CT scanner. Counts at 1 min intervals showed small standard deviations (e.g., mean values ± 1.0 for gray matter and likewise for white matter). Preliminary experience with the larger human brain indicates that anatomic regions of gray and white matter can be analyzed with greater reliability because of greater ease in identifying anatomic landmarks. Calculated LCBF values derived from very small regions of brain in the baboon using the in vivo autoradiographic algorithm were reproducible with $r = 0.89$, level of confidence of $p < 0.05\%$, and measurement error of 10.2 ± 4.1 . Local λ measurements showed a variation coefficient of 5.2 ± 1.9 . To achieve these values, it is imperative that head movement be avoided.

The anatomic regions examined were confirmed by comparison of the CT slices with those obtained at autopsy and were found to be anatomically correct. Similar to reports of local cerebral glucose use in the monkey [32], as judged by multiple simultaneous LCBF measurements of small regions of the brain, there was marked heterogeneity of regional rates of blood flow consistent with known histologic cytoarchitecture and local rates of metabolism and electrophysiologic function. There were striking differences in LCBF values between small neighboring structures of a few millimeters (e.g., caudate nucleus vs. internal capsule, cerebral cortex vs. subcortical white matter of the centrum semiovale, and high flow rates in the superior and inferior colliculi).

Scanning speeds of 1 min were certainly adequate for reliable sequential measurements of LCBF. From a practical clinical standpoint, LCBF values recorded at intervals of 1 min are satisfactory and a considerable improvement over intervals of 10 min currently required for ^{133}Xe measurements.

In summary, local cerebral blood flow and partition coefficient (λ) measurements with high resolution (0.04 mm^3) may be measured in vivo by brief inhalation of Xe^s while end-tidal Xe^s ($PEXe^s$) concentration is recorded with an inexpensive thermoconductivity detector and recording changes in Hounsfield units of brain tissue with the CT scanner at 1 min intervals. Because of reduced Compton scatter and tissue overlap, small zones of zero, high, and low perfusion (inhomogeneity of flow) are easily recognized with a resolution not previously possible. Pathologic changes in tissue which alter their solubility may also be quantified, and calculation of LCBF may be corrected for such changes in local λ . These measurements may be combined with activation techniques and/or with iodine contrast infusion to show changes in blood volume and/or the blood-brain barrier. Care should be taken to minimize radiation exposure and to avoid anesthetic effects induced by prolonged inhalation of high Xe^s concentrations.

ACKNOWLEDGMENTS

Walter Obrist, University of Pennsylvania, and Burton Drayer, Duke University, provided consultation, criticism, and advice during this project. Dr. Obrist provided the DEC 10 monoexponential

clearance program for calculating local cerebral blood flow (see footnote, p. 217). The computer program for solution of equation 6, as an in vivo autoradiographic method for calculating LCBF, was developed with the assistance of Shoichiro Nakamura, Ohio State University (see footnote, p. 217).

REFERENCES

1. Drayer BP, Wolfson SK Jr, Reinmuth OM, Dujovny M, Boehnke M, Cook TF. Xenon enhanced CT for analysis of cerebral integrity, perfusion and blood flow. *Stroke* 1978;9:123-130
2. Drayer B, Gur D, Wolfson S, Dujovny M. Regional blood flow in the posterior fossa. Xenon enhanced CT scanning. In: Gotoh F, Nagai H, Tazaki Y, eds. *Cerebral blood flow and metabolism. Acta Neurol Scand [Suppl 2]* 1979;60:218-219
3. Drayer BP, Wolfson SK, Rosenbaum AE, Dujovny M, Boehnke M, Cook EE. Comparative cranial CT enhancement in the normal primate. *Invest Radiol* 1979;14:88-96
4. Drayer BP, Dujovny M, Wolfson SK, Boehnke M, Cook EG, Rosenbaum AE. Comparative cranial CT enhancement in a primate model of cerebral infarction. *Ann Neurol* 1979;5:48-58
5. Kelcz F, Hilal SK, Hartwell P, Joseph PM. Computed tomographic measurement of the xenon brain-blood partition coefficient and implication for regional cerebral blood flow: a preliminary report. *Radiology* 1978;127:385-392
6. Meyer JS, Yamamoto M, Hayman LA, Sakai F, Nakajima S, Armstrong D. Cerebral embolism: local CBF and edema measured by CT scanning and Xe inhalation. Submitted for publication
7. Collins V. Pharmacology of inorganic gas anesthetic xenon. In: *Principles of anesthesiology*, 2d ed. Philadelphia: Lea & Febiger, 1976:1541-1542
8. Cullen SC, Gross EG. The anesthetic properties of xenon in animals and human beings, with additional observations on krypton. *Science* 1951;113:580-582
9. Foley WD, Haughton VM, Schmidt J, Wilson CR. Xenon contrast enhancement in computed body tomography. *Radiology* 1978;129:219-220
10. Morris LE, Knott JR, Pittinger CB. Electroencephalographic and blood gas observations in human surgical patients during xenon anesthesia. *Anesthesiology* 1955;16:312-319
11. Pittinger CB, Faulconer A, Knott JR, Pender JW, Morris LE, Bickford RG. Electroencephalographic and other observations in monkeys during xenon anesthesia at elevated pressures. *Anesthesiology* 1955;16:551-563
12. Pittinger CB, Moyers J, Cohen SC, Featherstone RM, Gross EG. Clinicopathologic studies associated with xenon anesthesia. *Anesthesiology* 1953;14:10-17
13. Pittinger CB, Featherstone RM. Xenon concentration in brain and other body tissue. *J Pharmacol Exp Ther* 1954;70:110-118
14. Steward A, Allott PR, Cowles AC, Mapleson WW. Solubility coefficients for inhaled anesthetics for water, oil and biological media. *Br J Anaesthesiol* 1973;45:282-293
15. Ono H, Morijama T, Mori K. Measurement of regional cerebral blood flow by sequential xenon enhanced CT scan. In: Gotoh F, Nagai H, Tazaki Y, eds. *Cerebral blood flow and metabolism. Acta Neurol Scand [Suppl 2]* 1979;60:220-221
16. Duboulay GH, Radu EW, Thomas DJ, Kendall BE. Plain, iohalamate-enhanced and xenon-enhanced CT in cerebral infarction. In: Nelson E, Price TR, eds. *Cerebrovascular diseases*, 11th Princeton conference. New York: Raven, 1979: 57-69
17. Computer assisted tomography in nontumoral diseases of the

- brain, spinal cord and eye. In: Di Chiro G, Brooks RA, eds. *Proceedings of the International Conference*. Bethesda: National Institutes of Health, 1976
18. Winkler SS, Sackett JF, Holden JE, Flemming DC, Alexander SC, Madsen M, Kimmel RI. Xenon inhalation as an adjunct to computerized tomography of the brain: preliminary study. *Invest Radiol* 1977;12:15-18
 19. Radne EW, Kendall BE. Iodide and xenon enhancement of computer tomography (CT) in multiple sclerosis. *Neuroradiology* 1978;15:153-158
 20. Veall N, Mallett BL. The partition of trace amounts of xenon between human blood and brain tissues at 37°C. *Phys Med Biol* 1965;10:375-380
 21. Eichling JO, Ter-Pogossian MM. Methodological shortcomings of the ^{133}Xe inhalation technique of measuring rCBF. In: Ingvar DH, Lassen NA, eds. *Cerebral function, metabolism and circulation*. *Acta Neurol Scand [Suppl 64]* 1977;56:464-465
 22. Obrist WD, Thompson HK, Wang HS, Wilkinson WE. Regional cerebral blood flow estimated by ^{133}Xe inhalation. *Stroke* 1975;6:245-256
 23. Meyer JS, Ishihara N, Deshmukh VD, et al. Improved method for noninvasive measurement of regional cerebral blood flow by ^{133}Xe inhalation. *Stroke* 1978;9:195-203
 24. Kanno I, Lassen NA. Two methods for calculating regional cerebral blood flow for emission computed tomography of inert gas concentrations. *J Comput Assist Tomogr* 1979;3:71-76
 25. Hayman LA, Sakai F, Meyer JS, Armstrong D, Hinck VC. Iodine-enhanced CT patterns after cerebral arterial embolization in baboons. *Am J Neuroradiol* 1980;1:233-238
 26. Sakai F, Meyer JS, Yamaguchi F, Yamamoto M, Shaw T. ^{133}Xe inhalation method for measuring cerebral blood flow in conscious baboons. *Stroke* 1979;10:310-318
 27. Kety SS. Measurement of local blood flows by the exchange of inert, diffusible substance. In: Bonner HO, ed. *Methods in medical research*, vol 8. Chicago: Year Book, 1960:228-238
 28. Kety SS, Schmidt CF. The nitrous oxide method for quantitative determination of cerebral blood flow in man; theory, procedure and normal values. *J Clin Invest* 1948;27:476-483
 29. Landau WM, Freygang WH Jr, Noland LP, Sokoloff L. The local circulation of the living brain, values in the unanesthetized and anesthetized cat. *Trans Am Neurol Assoc* 1955;80:125-129
 30. Reivich M, Jehle J, Sokoloff L, Kety SS. Measurement of regional cerebral blood flow with antipyrine- ^{14}C in awake cats. *J Appl Physiol* 1969;27:296-300
 31. Pasztor E, Symon L, Dorsch NWC, Branston NM. The hydrogen clearance method in assessment of blood flow in cortex, white matter and deep nuclei of baboons. *Stroke* 1972;4:556-567
 32. Kennedy C, Sakurada O, Shinohara M, Jehle J, Sokoloff L. Local cerebral glucose utilization in the normal conscious macaque monkey. *Ann Neurol* 1978;4:293-301
 33. Yamamoto M, Meyer JS, Sakai F, Yamaguchi F, Jacoby R, Shaw T. Mechanisms of cerebral vasomotor responsiveness to carbon dioxide in health and disease. In: Meyer JS, Lechner H, Reivich M, eds. *Cerebral vascular disease*, proceedings of the 9th International Salzburg Conference. Amsterdam: Excerpta Medica, 1979:280-286